Cosmic rays and supernova remnants:
e-ASTROGAM perspective

Andrei Bykov
Ioffe Institute St.Petersburg

Particle acceleration and GCR origin

MeV-GeV emission from cosmic ray accelerators

SNRs: Injection of leptonic CR component

Superbubbles?

The Crab Nebula & the Vela PWN

Source distributions

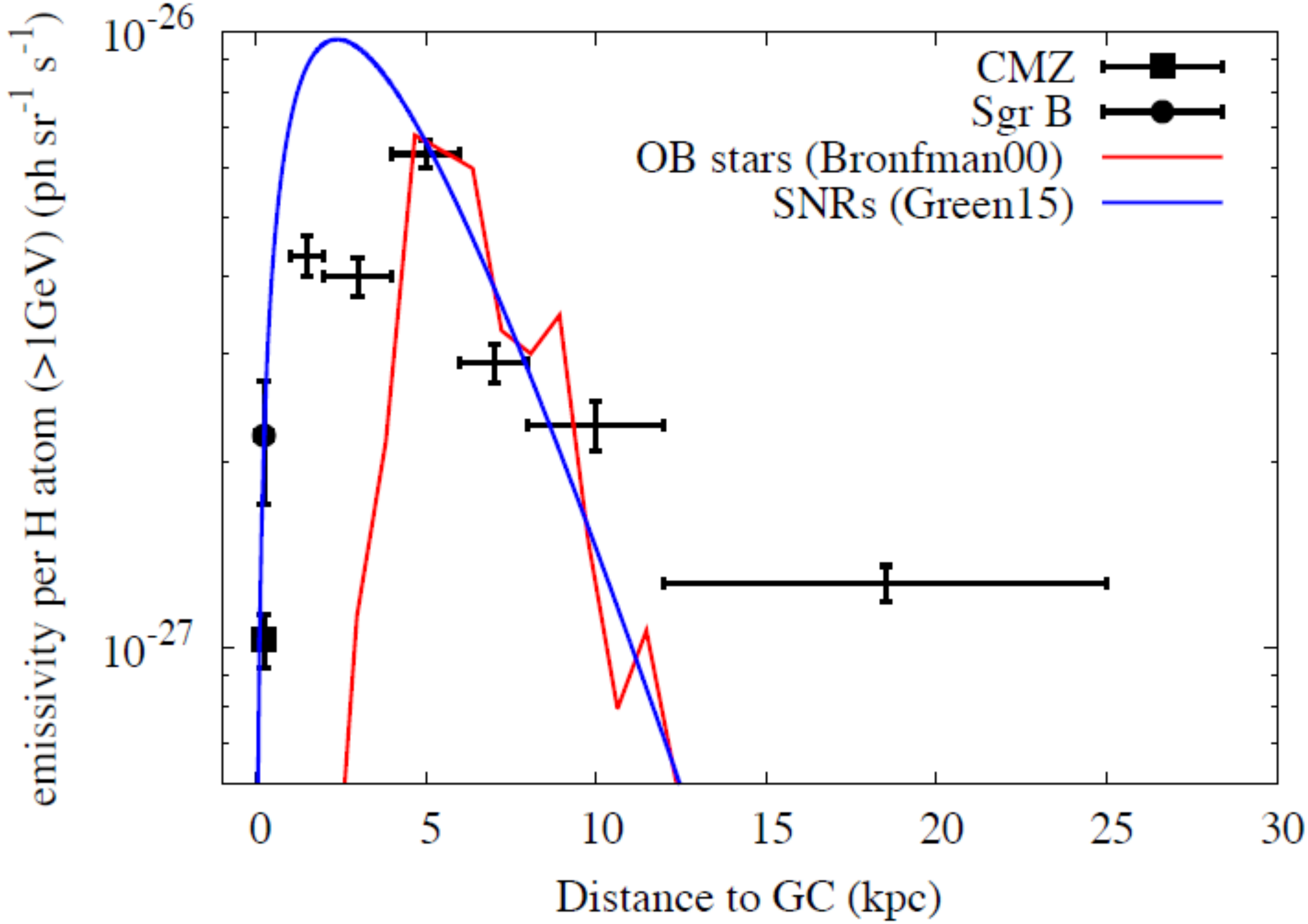

Peak coincide with OB stars

R.Yang+2016

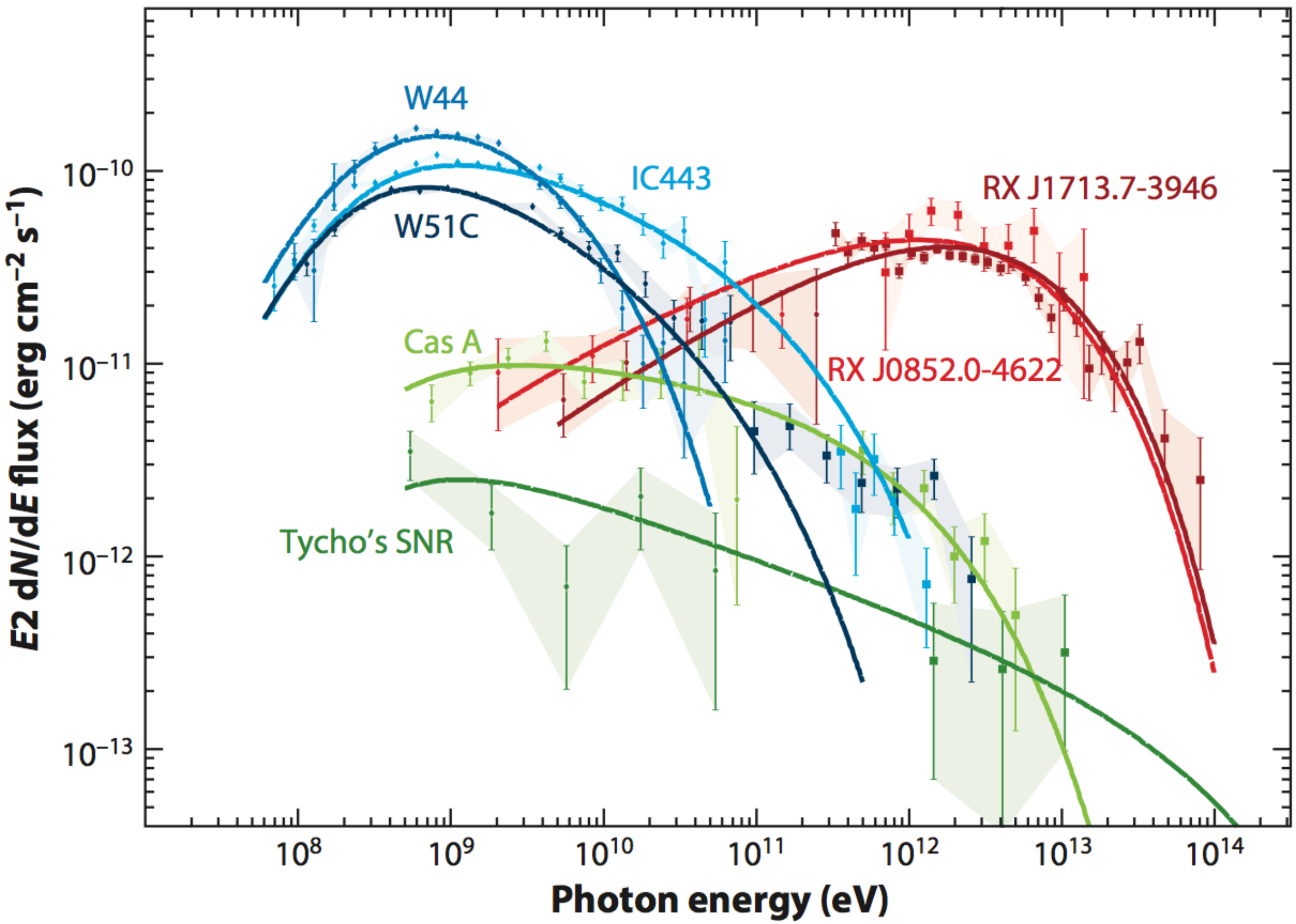

S. Funk 2015

- ***What are the sources of PeV regime CRs?***

MeV-GeV emission from cosmic ray accelerators:

Young Galactic SNRs

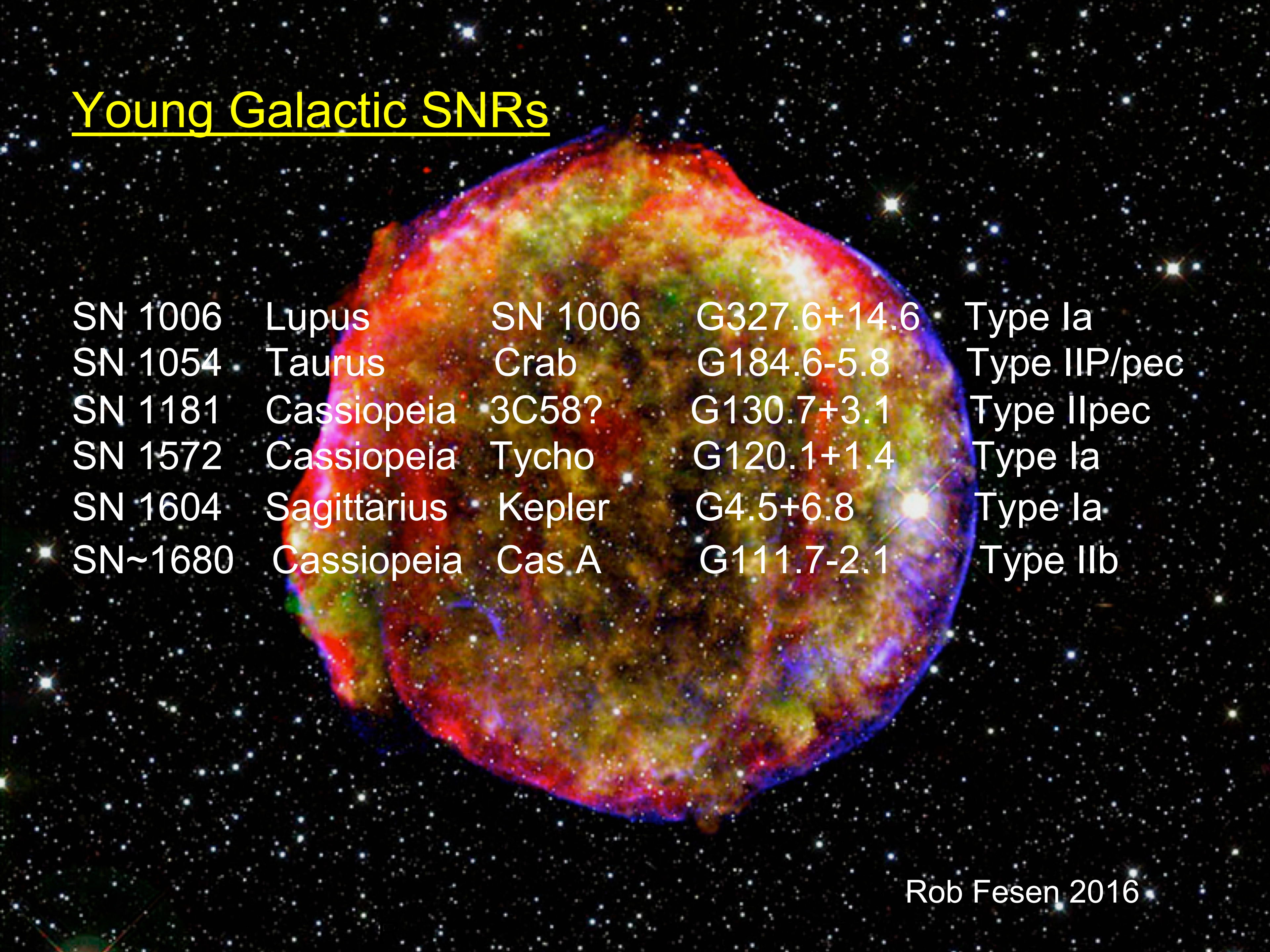

Young Galactic SNRs

SN 1006	Lupus	SN 1006	G327.6+14.6	Type Ia
SN 1054	Taurus	Crab	G184.6-5.8	Type IIP/pec
SN 1181	Cassiopeia	3C58?	G130.7+3.1	Type IIpec
SN 1572	Cassiopeia	Tycho	G120.1+1.4	Type Ia
SN 1604	Sagittarius	Kepler	G4.5+6.8	Type Ia
SN~1680	Cassiopeia	Cas A	G111.7-2.1	Type IIb

Rob Fesen 2016

X-ray image of Cas A

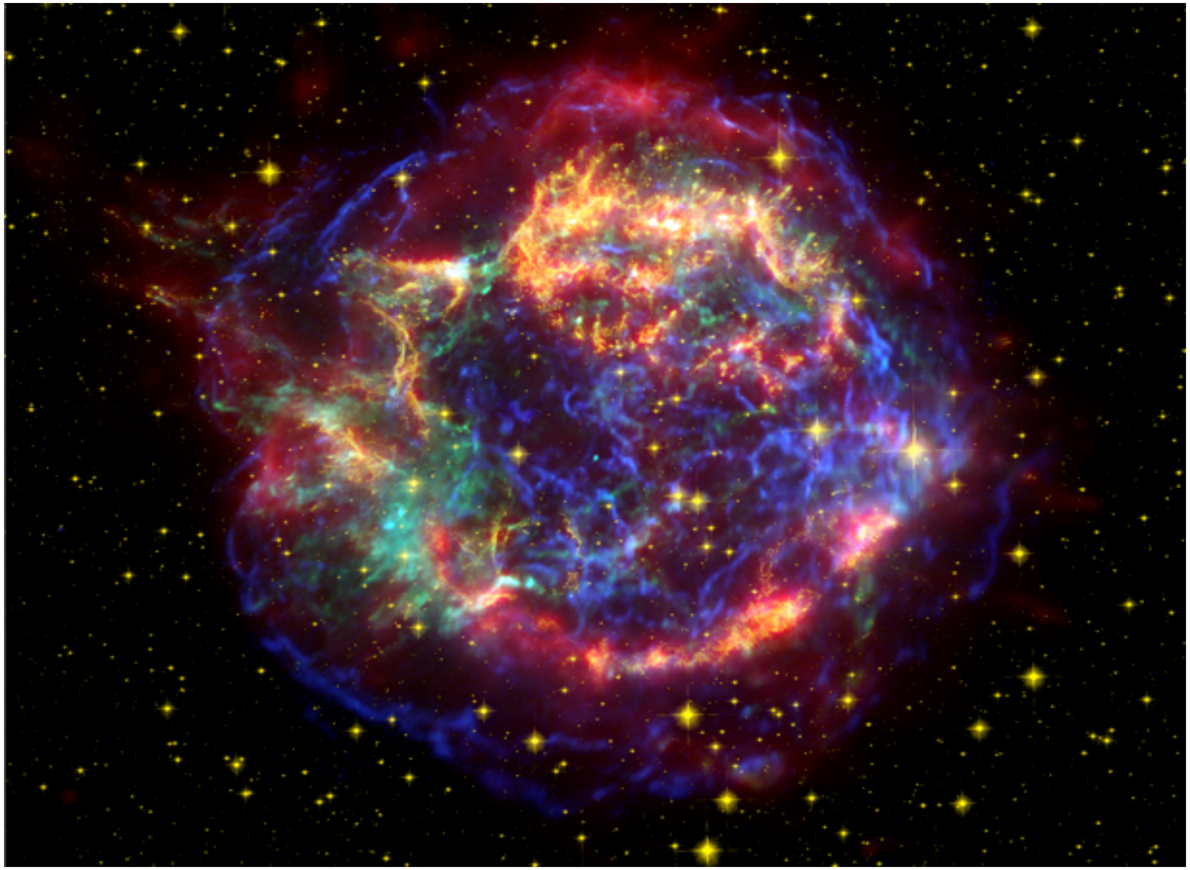

Chandra CXO

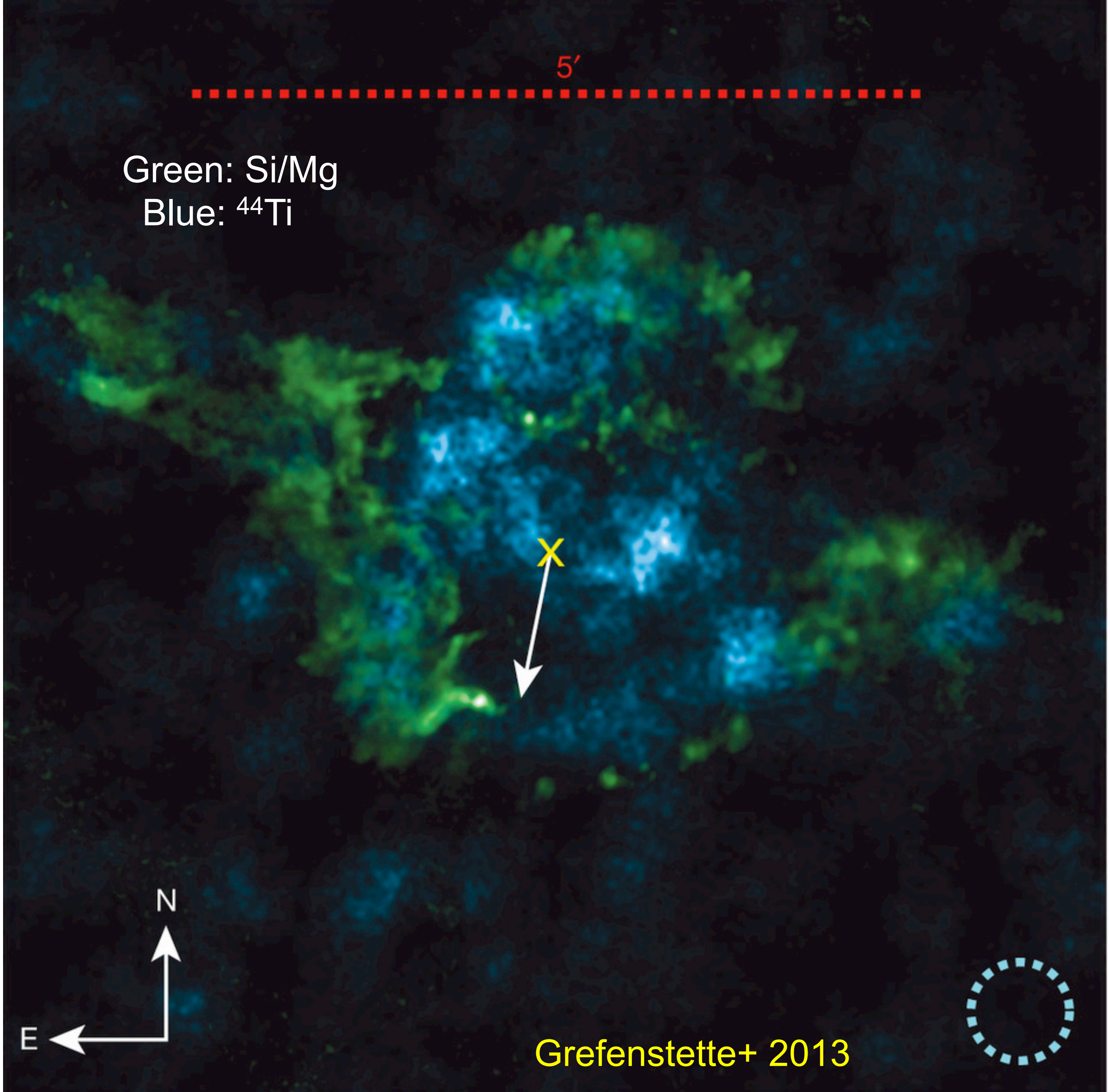
5′
Green: Si/Mg
Blue: ^{44}Ti
X
N
E
Grefenstette+ 2013

Cas A continuum spectrum: electron injection constrains

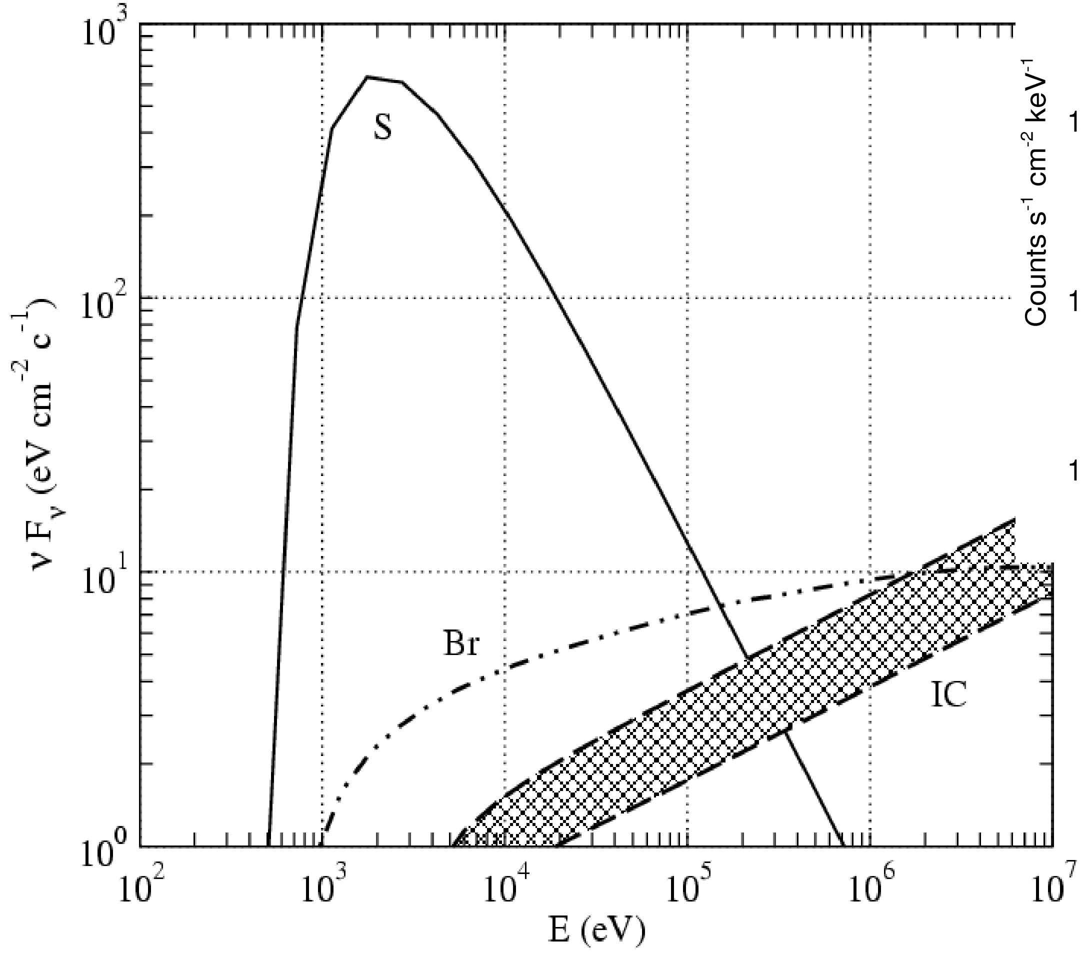

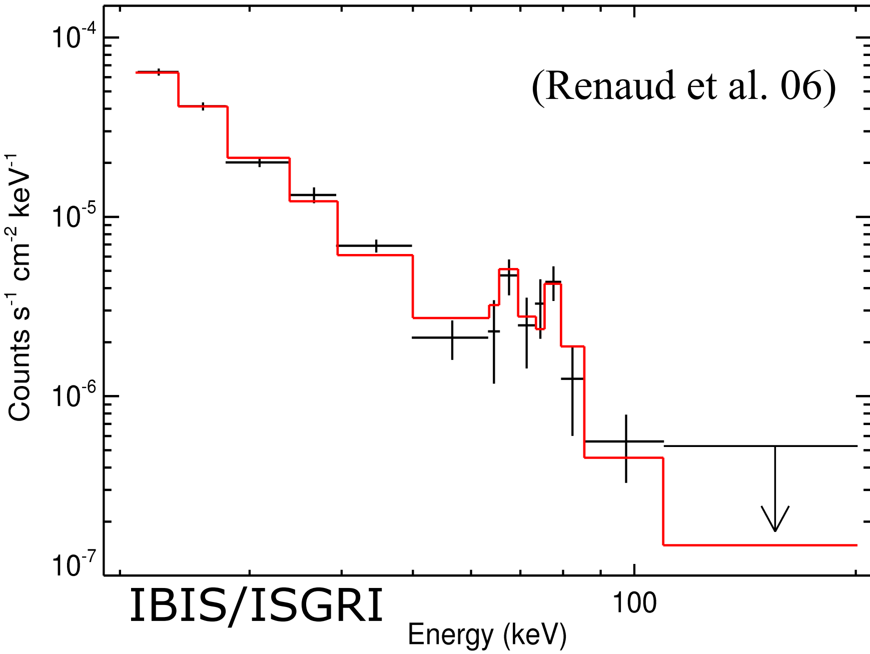

IBIS/ISGRI

AB+

MeV-GeV emission from cosmic ray accelerators:

SNR in molecular clouds
Slow shocks 100-200 km/s…

Fermi images of “molecular” SNRs

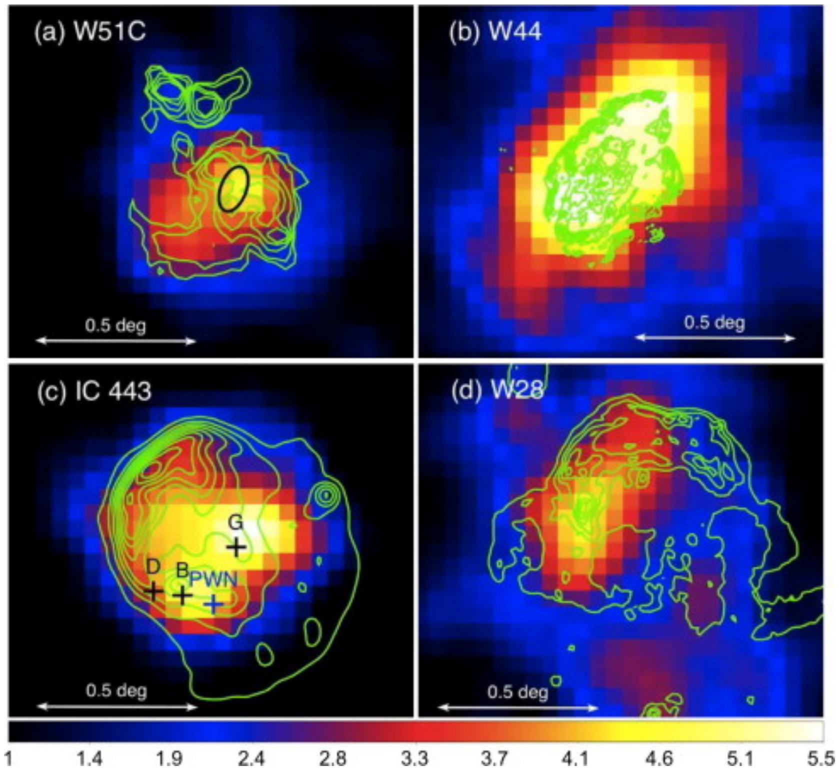

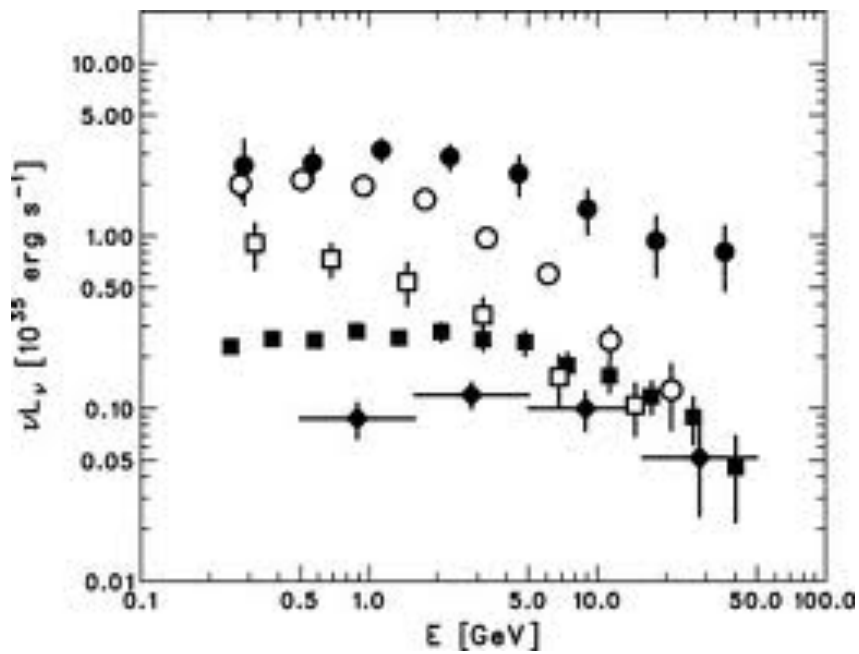

$$L_\gamma \sim 10^{34} - 10^{36} erg/s$$

W51C (filled circles) W44 (open circles);
IC 443 (filled rectangles); W28 (open rectangles)
Cassiopeia A (filled diamonds).

Thompson Baldini Uchiyama 2012

SNR in Molecular Clouds

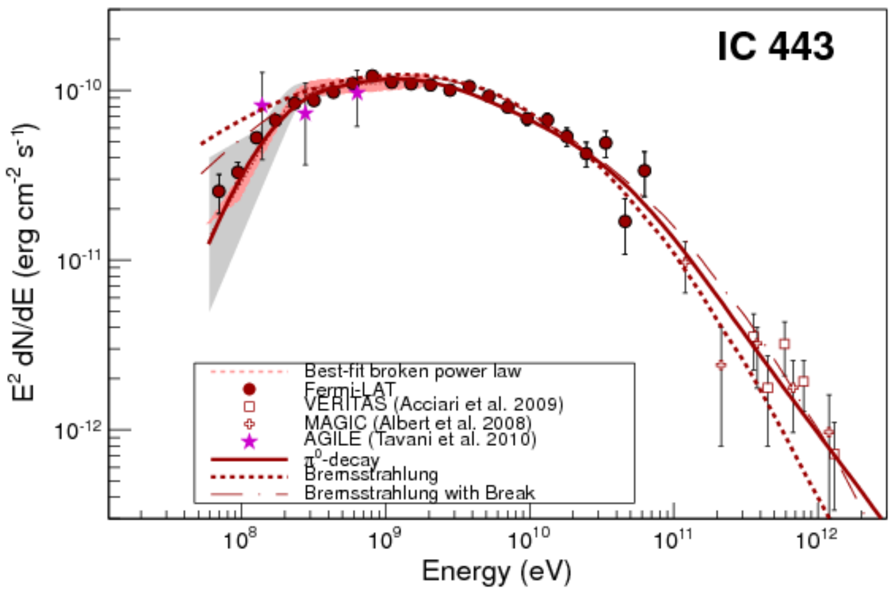

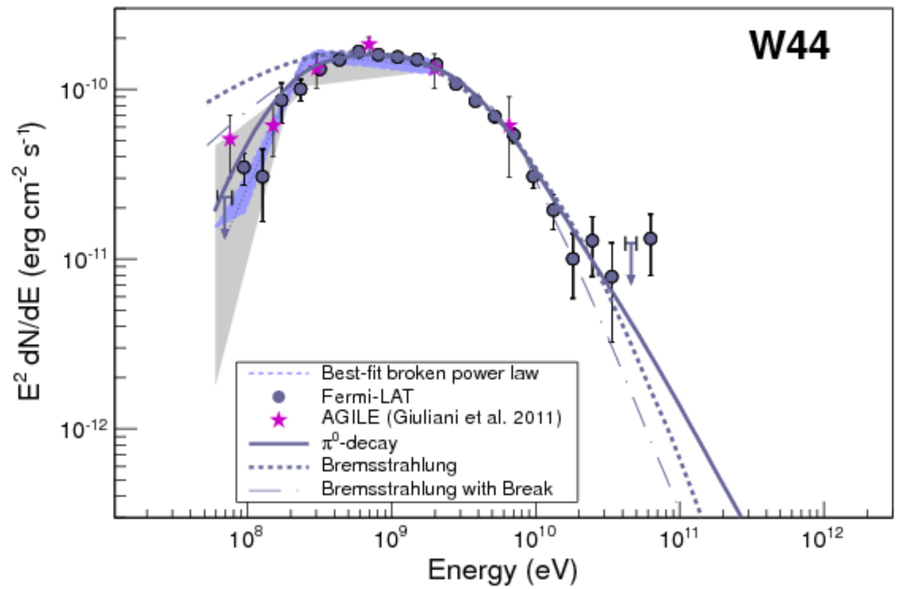

M.Ackermann 2013

Pion-Decay Signatures

see: Tavani + 2010, Uchiyama+ 2010, Giuliani+ 2011, Ackermann+ 2013, Cardillo+ 2014

XMM 2-8 keV -- 24 mum IC 443

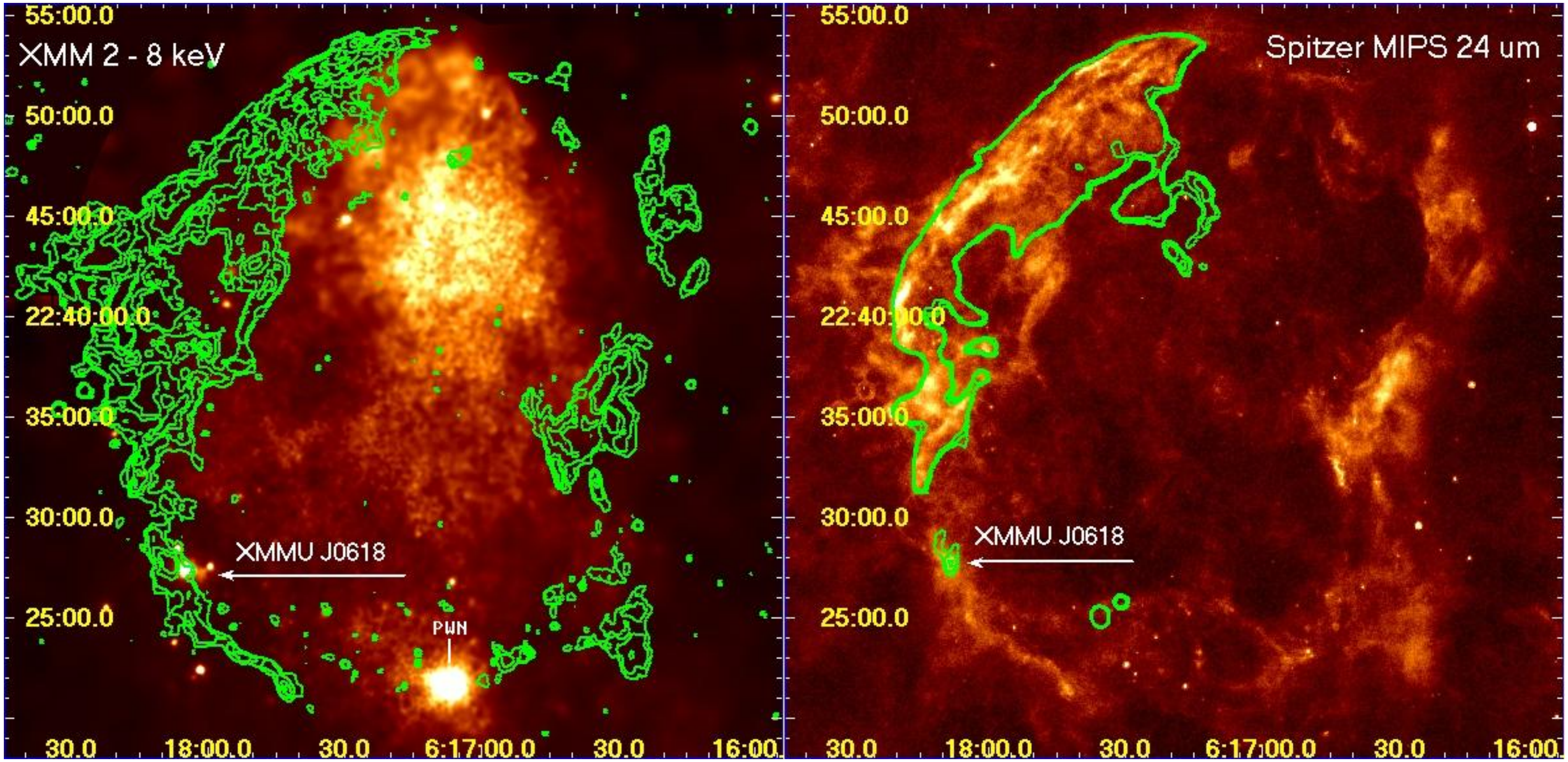

BKUBBDGP 2008

LECR? Ionization rate

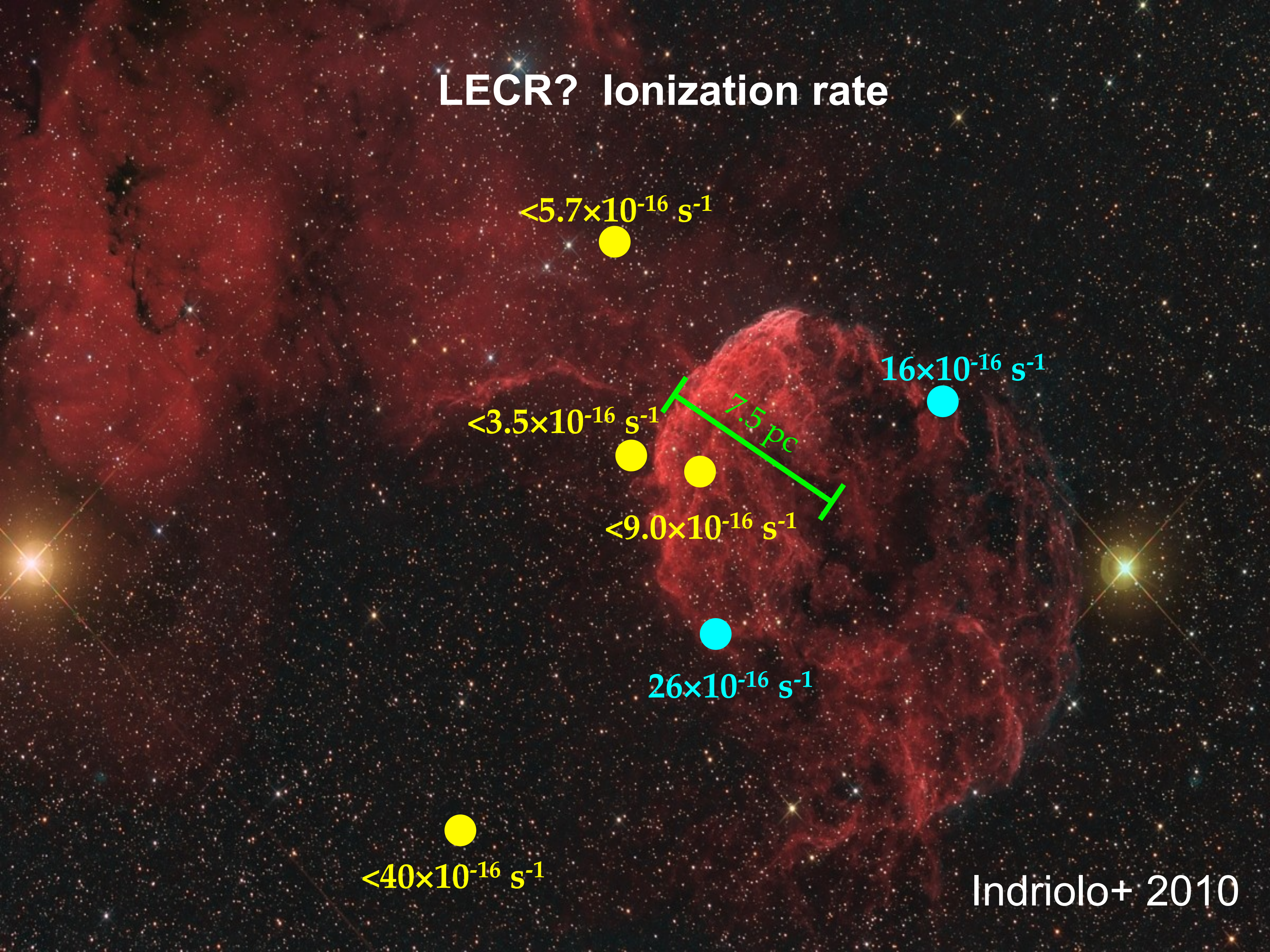

Indriolo+ 2010

CR re-acceleration in molecular SNR (energetically efficient)

THE ASTROPHYSICAL JOURNAL, 800:103 (10pp), 2015 February 20

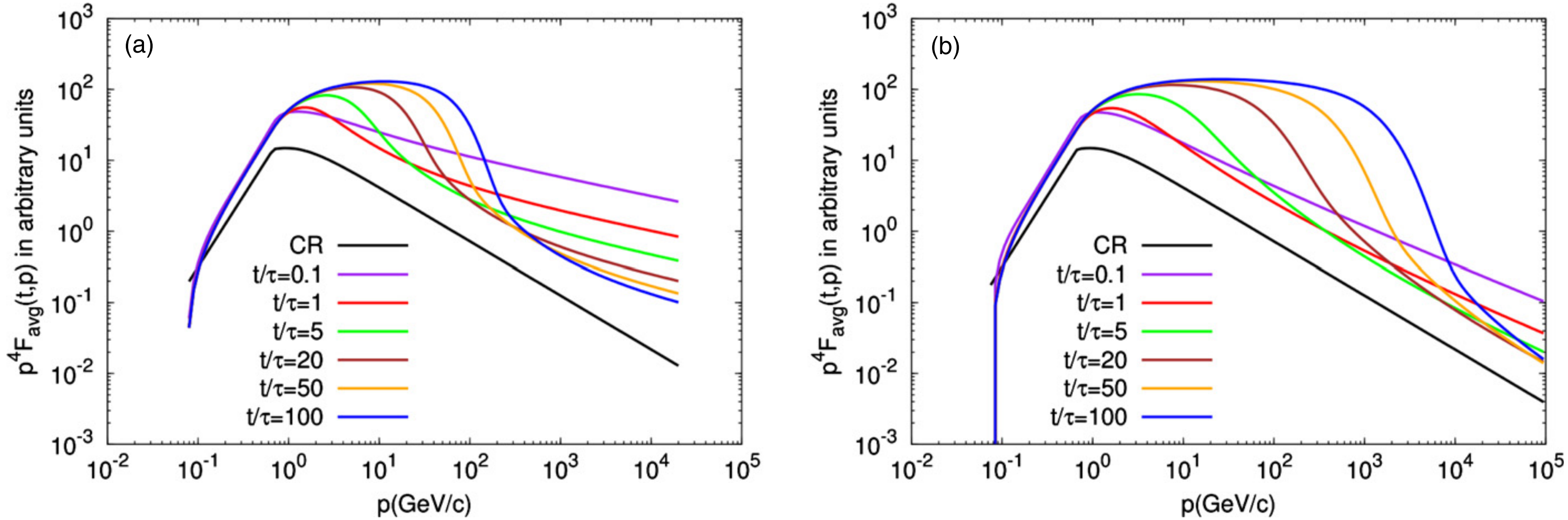

Figure 3. Time evolution of the spatially averaged downstream particle momentum spectrum. The cosmic-ray spectrum denoted by CR has arbitrary scaling. (a) Bohm-like diffusion with diffusion coefficient $\kappa \propto p$; (b) diffusion coefficient $\kappa \propto p^{0.5}$.

CR compression CR re-acceleration CR transport cloud-shell

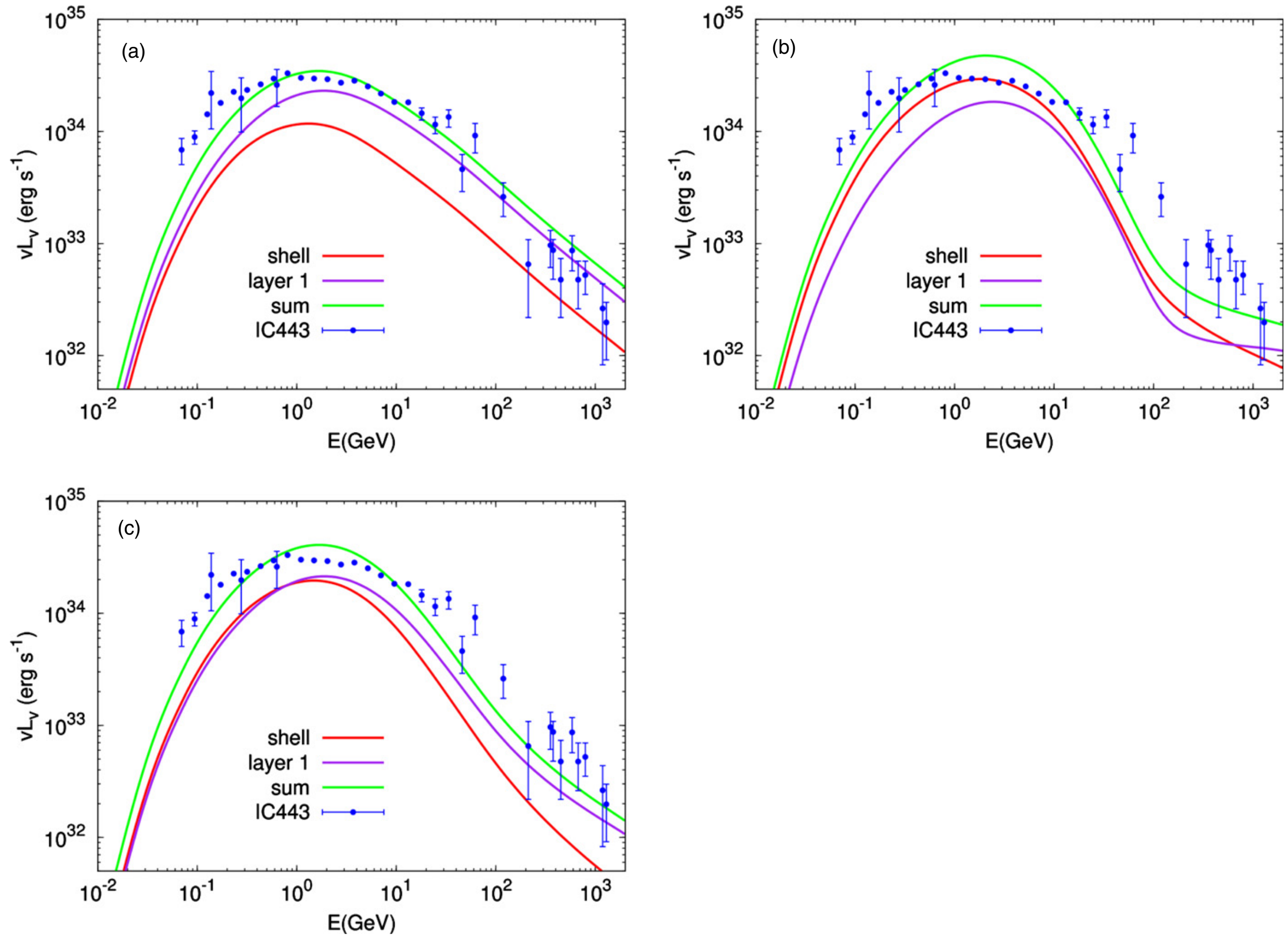

Figure 4. π^0-decay emission from IC 443 for different energy dependence of the diffusion coefficient. Shell is the radiative shell of the remnant, layer 1 is the shocked shell, and sum is the sum of the two components. (a) Energy-independent diffusion with $\theta_f = 2\theta_{l_1} = 2$ at $p = 1\,\mathrm{GeV}\,c^{-1}$ and $\eta = 0.2$ compared to observations; (b) energy-dependent diffusion with $\kappa \propto p$, $\theta_f = \theta_{l_1} = 40$ at $p = 1\,\mathrm{GeV}\,c^{-1}$ and $\eta = 0.06$; (c) energy-dependent diffusion with $\kappa \propto p^{0.5}$, $\theta_f = 16\theta_{l_1} = 8$ at $p = 1\,\mathrm{GeV}\,c^{-1}$ and $\eta = 0.15$. The data points are taken from the same references as in Tang & Chevalier (2014).

CR compresion vs CR re-acceleration

Cardillo + 2016

A&A 595, A58 (2016)

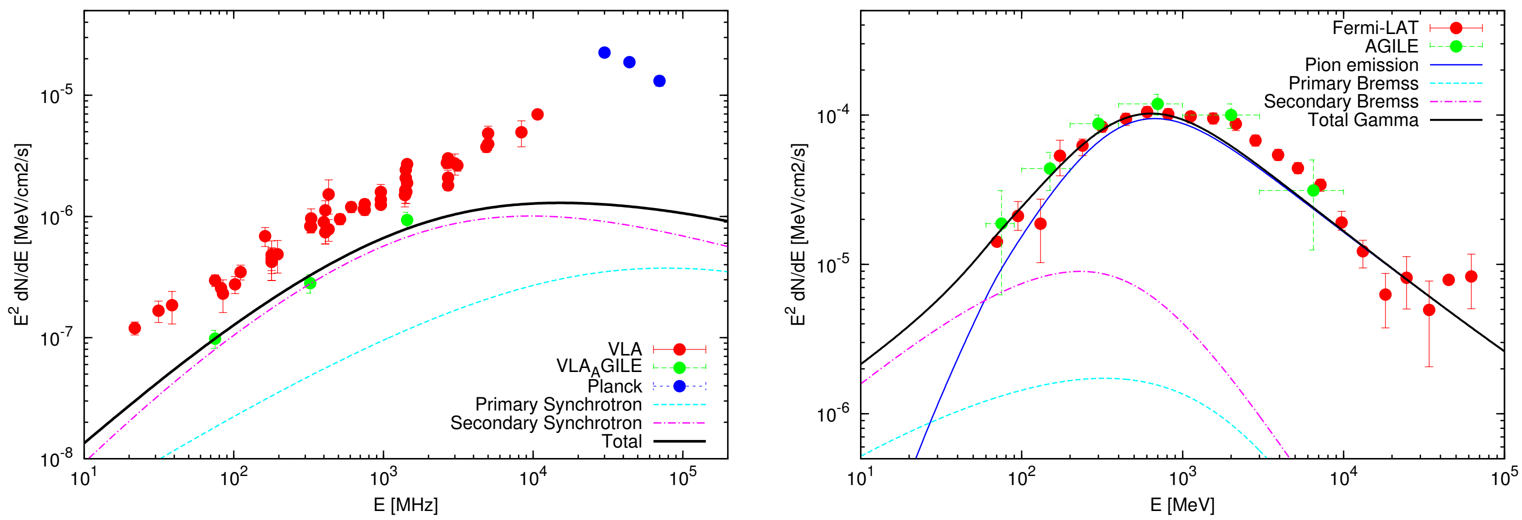

Fig. 5. Radio and γ-ray emission from SNR W44 assuming that Galactic CRs are only compressed at the shock and in the crushed cloud. In the *left (right) panel* we show the radio (γ ray) emission. Data are as in Fig. 3.

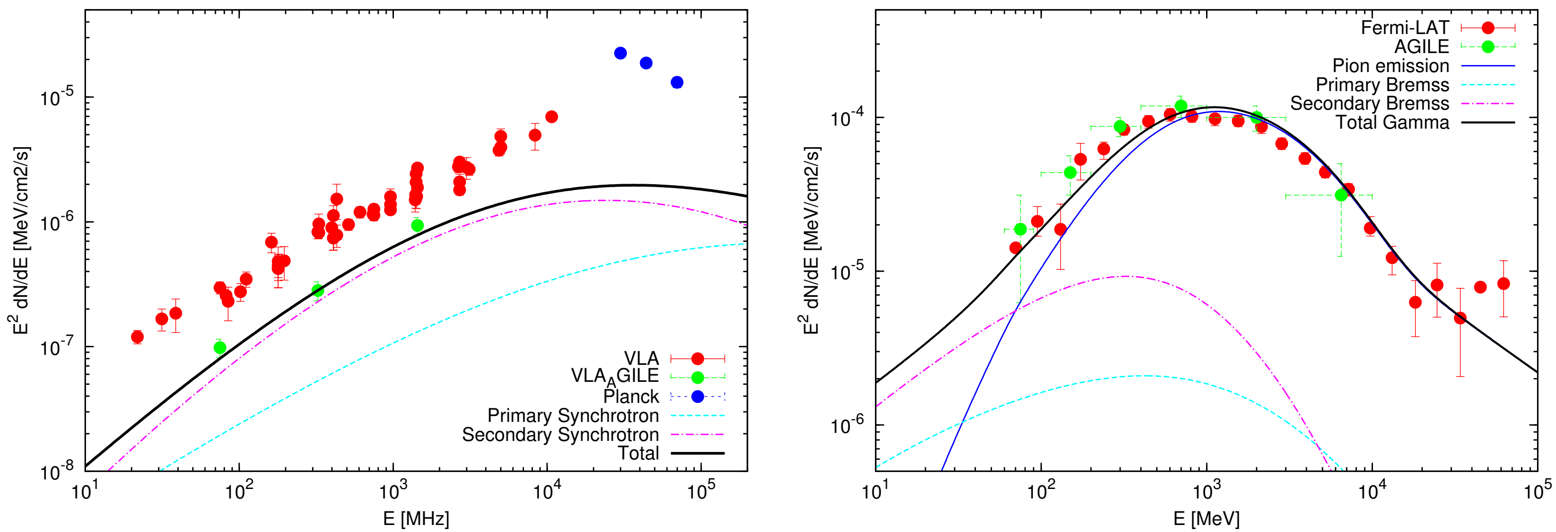

Fig. 3. *Left*: VLA (red) and *Planck* (blue) radio data from the whole remnant (Castelletti et al. 2007; Planck Collaboration Int. XXXI 2016) and VLA radio data from the high-energy emitting region (green), plotted together with primary (cyan dashed line), secondary (magenta dot-dashed line), and total (black line) synchrotron radio emission obtained in our best fit reacceleration model. *Right*: AGILE (green) and *Fermi*-LAT (red) γ-ray points (Cardillo et al. 2014; Ackermann et al. 2013) plotted with γ-ray emission from pion decay (blue dotted line), emission due to bremsstrahlung of primary (cyan dashed line), and secondary (magenta dot-dashed line) electrons, and total emission (black line).

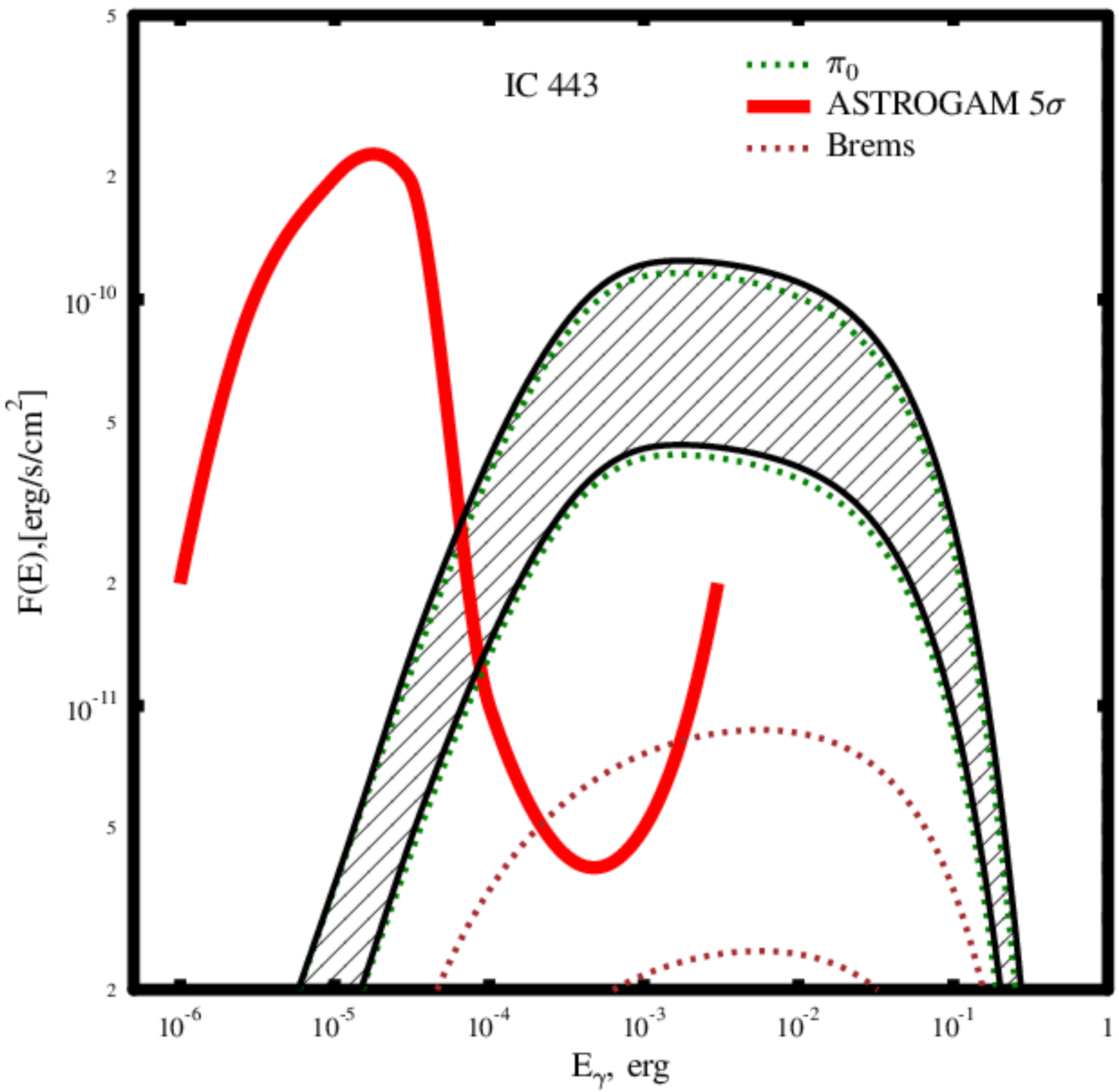

What can we learn with e-ASTROGAM:

Low energy CR background

Ionization starforming cloud

CR lepton/proton ratio in the sources

Physics of injection

Particle acceleration and GCR origin

Superbubbles?

SB around NGC 1929 in LMC VLT image

ESA/VLT Mejias

Fermi image of Cygnus superbubble

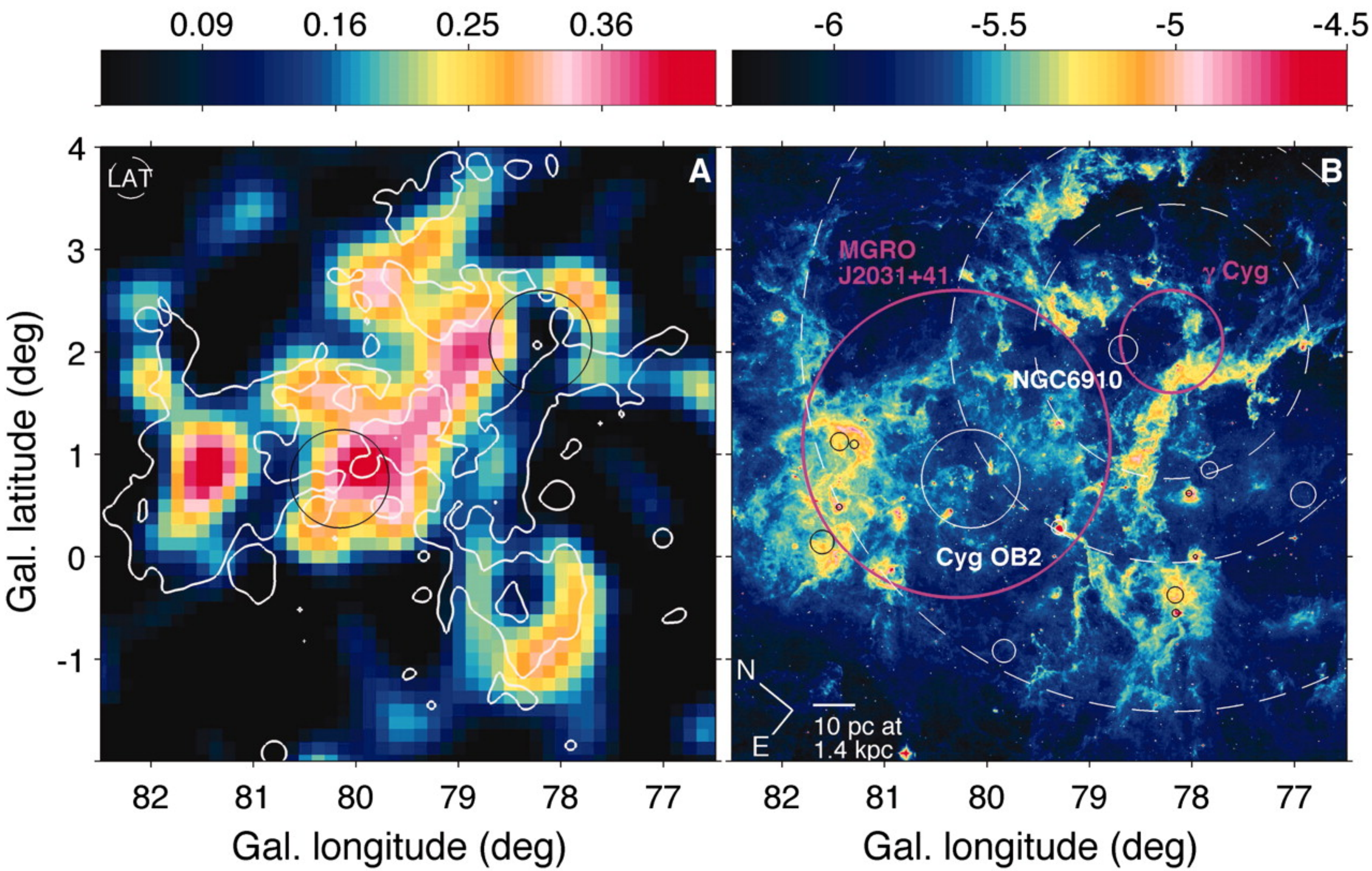

Ackermann + 2011

The Fermi source is extended of about 50 pc scale size and anti-correlate with MSX

Cygnus X is about 1.5 kpc away. Contain a number of young star clusters and several OB associations. Cygnus OB2 association contains 65 O stars and more than 500 B stars. There is a young supernova remnant Gamma-Cygni and a few gamma-pulsars.

Fermi image of Cygnus

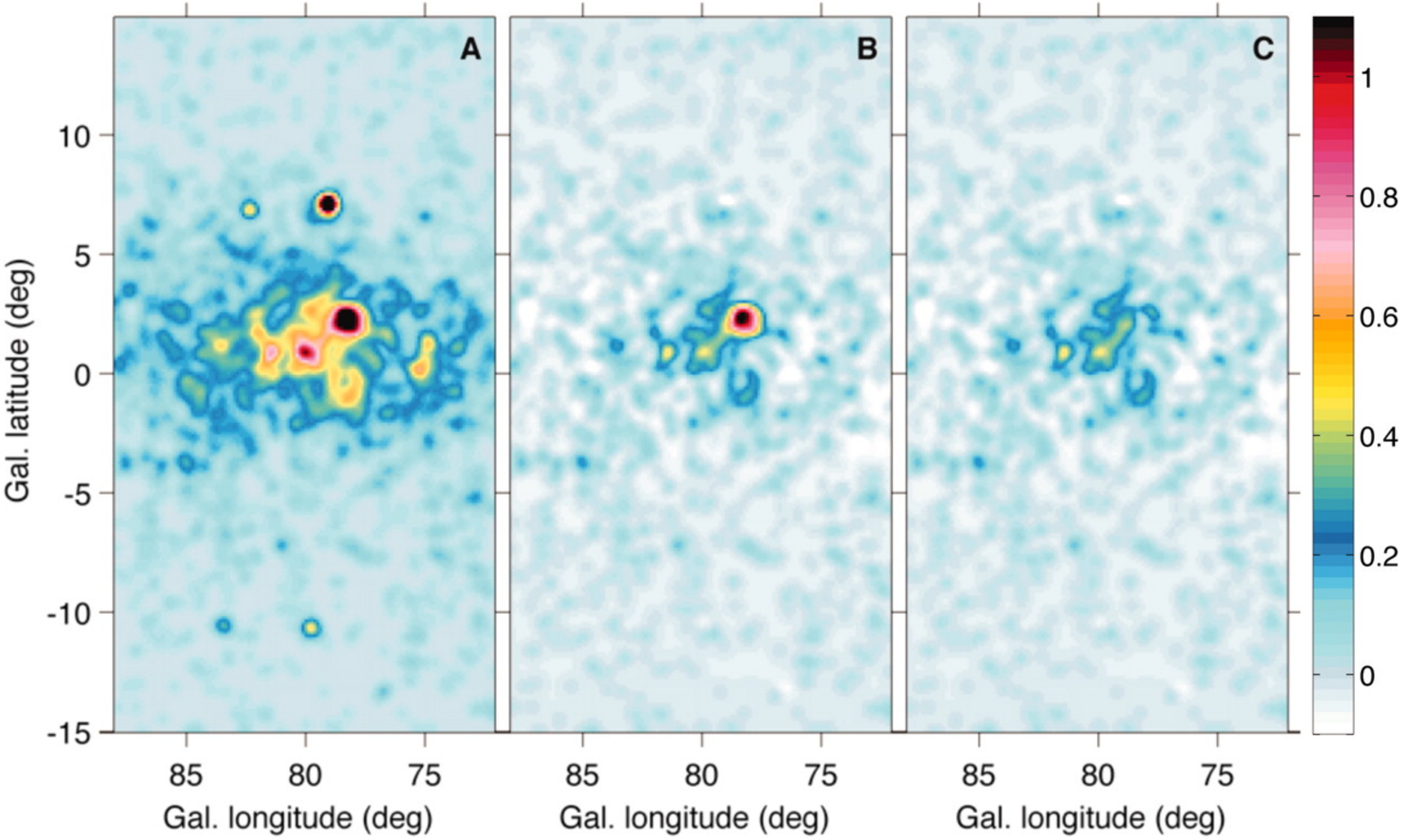

Ackermann + Science 2011

Fermi spectrum of Cygnus superbubble

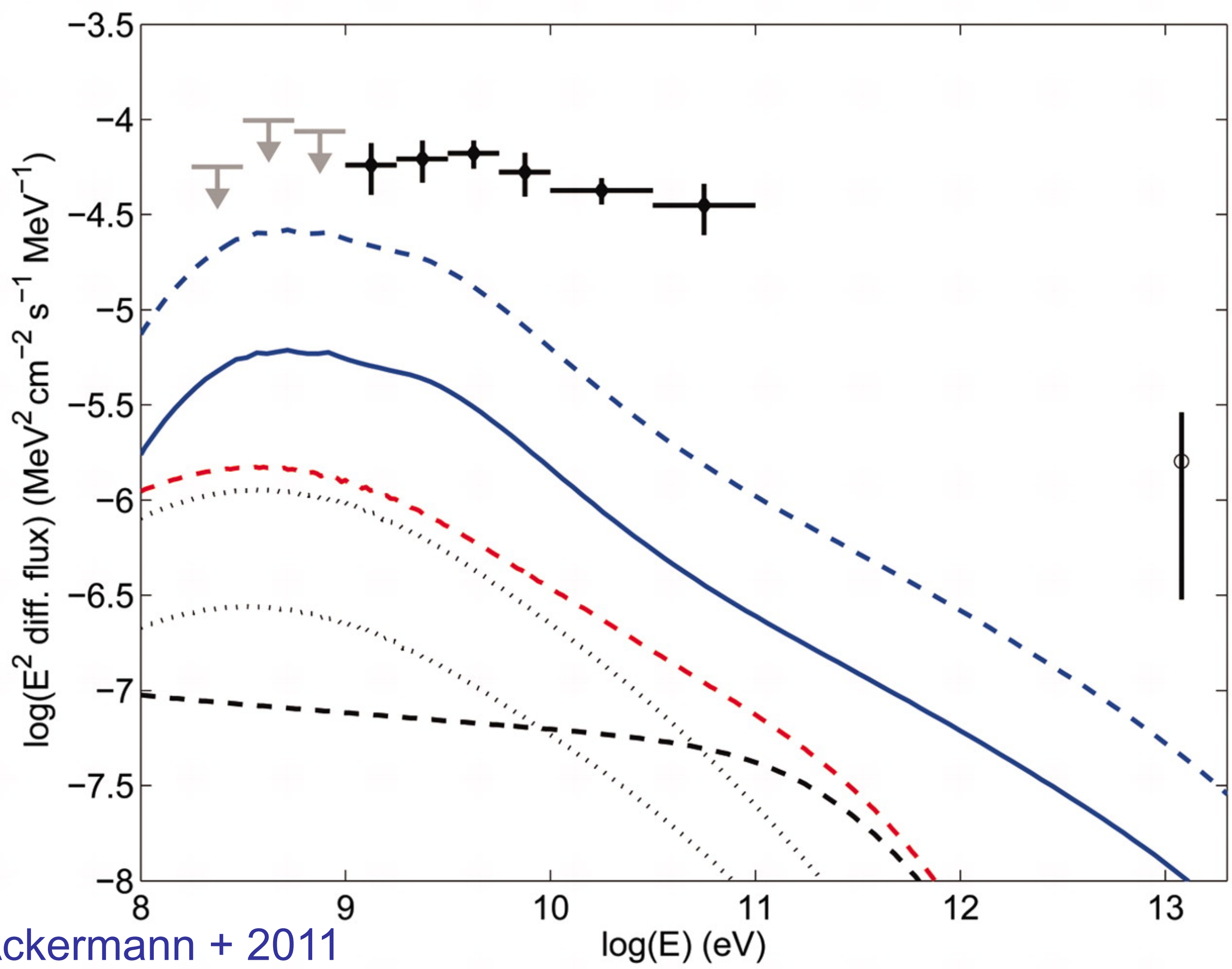

Ackermann + 2011

LECR Spectra in a SB

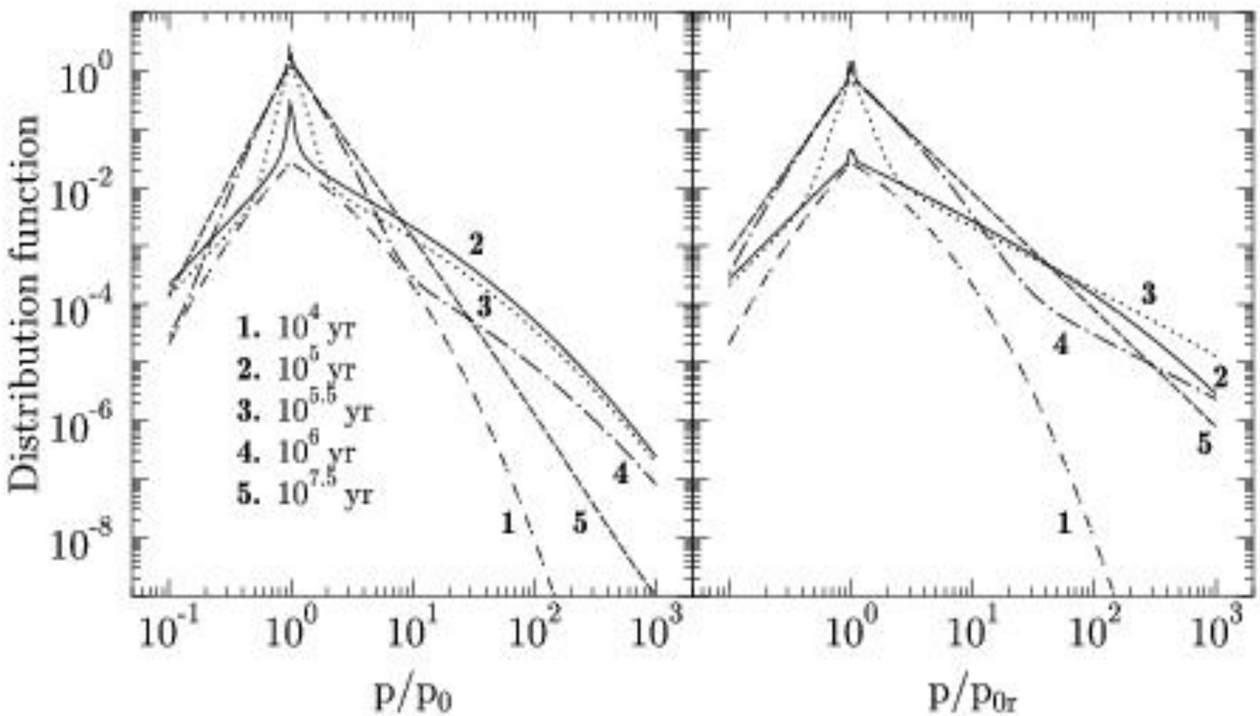

Space Sci. Rev. v.99, 317

Long-time LECR spectra evolution in SB

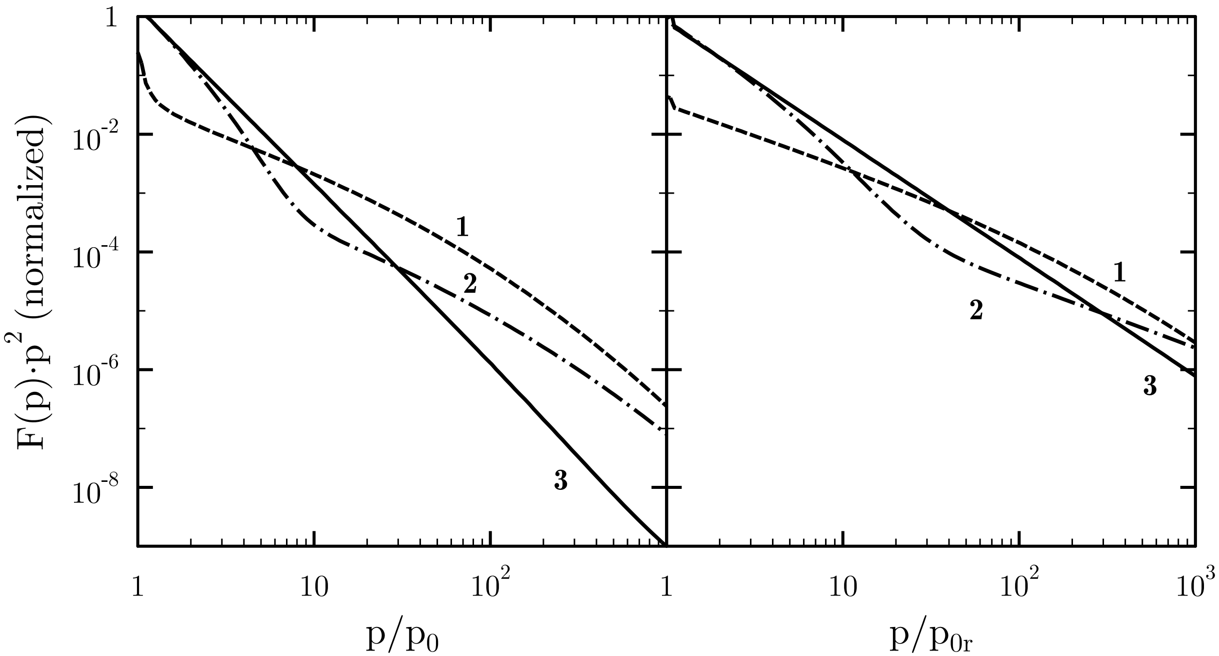

A&ARv v.22, 77, 2014

Low energy CRs accelerated by multiple compressive waves in the Solar Wind
by L. A. Fisk and G.Gloeckler 2014

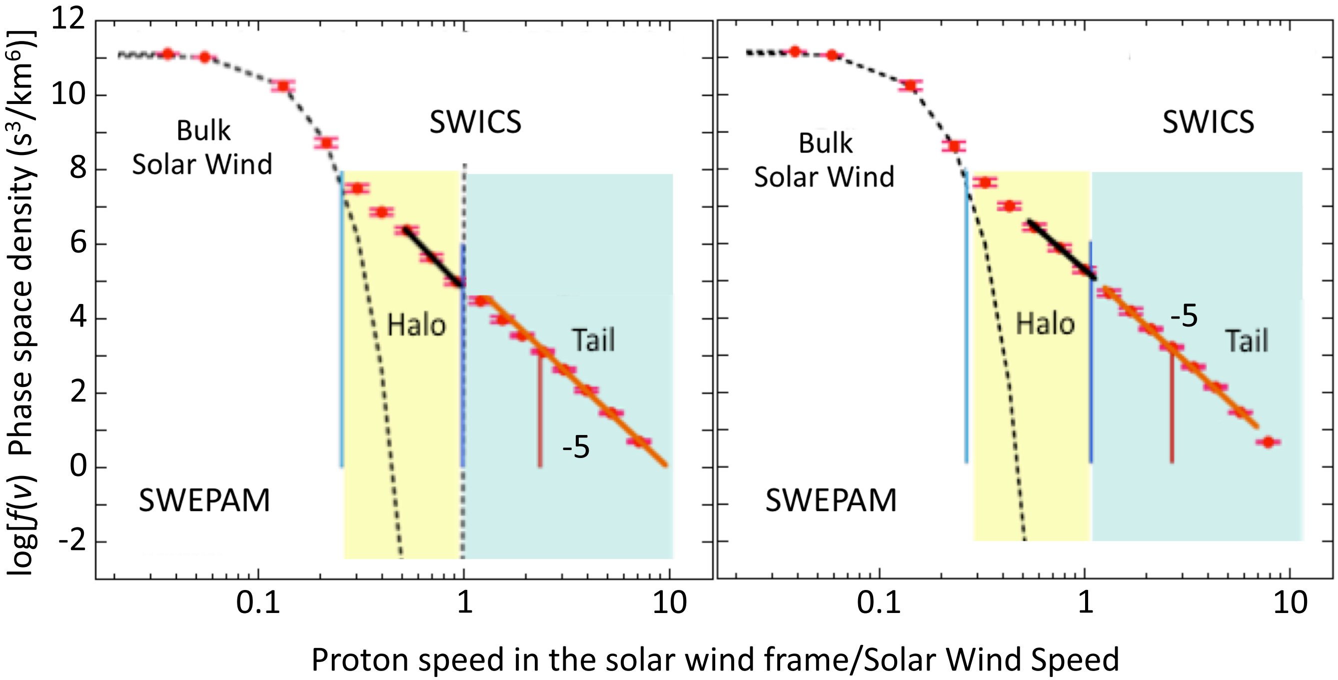

Figure 3. One-hour averaged solar wind frame velocity distribution functions showing the proton bulk solar wind, the halo and the tail segments during hour 11 of August 12, 2001, during which the strong (compression ratio of 3.85 ±0.15) shock passed *ACE* (left panel) and during the hour of peak tail density that was observed one hour downstream of the shock (right panel) (from [29]).

CR spectra in HI shell

NONTHERMAL PARTICLES IN H I SHELLS 505

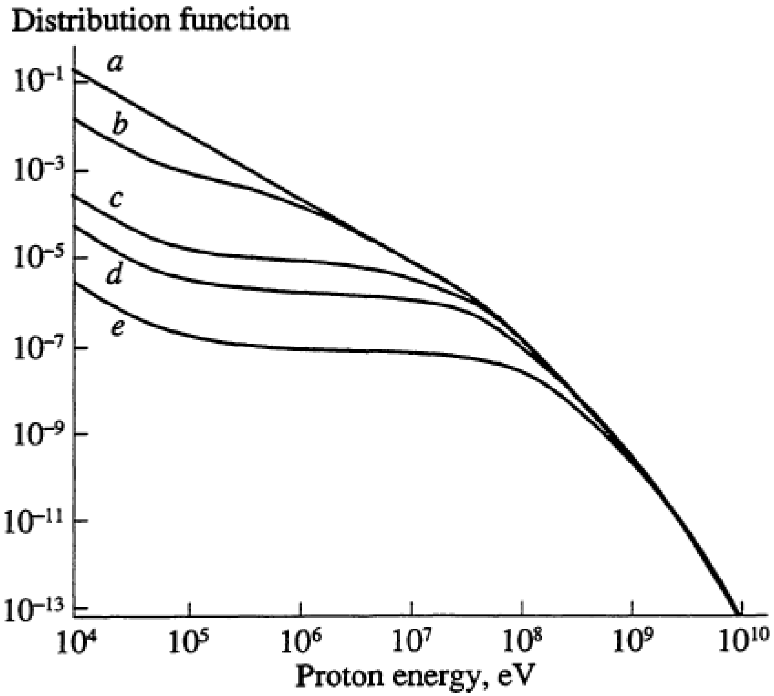

Fig. 1. The proton-spectrum variation with the shell's depth. Curves *a* - *e* are for dimensionless depths z = 0, 15, 300, 1000, and 5000, respectively.

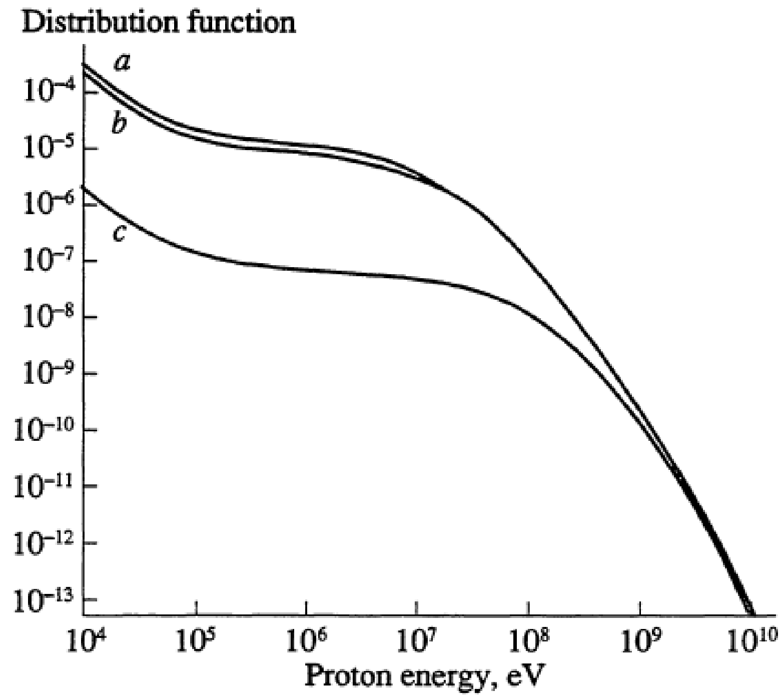

Fig. 2. The dependence of the proton spectrum at $z = 300$ on the character of particle transfer. Curve *a* is for $D(p) = \text{const}$; *b* and *c* correspond to $\alpha = 0.33$ and 0.5.

MeV-line spectra of a SB

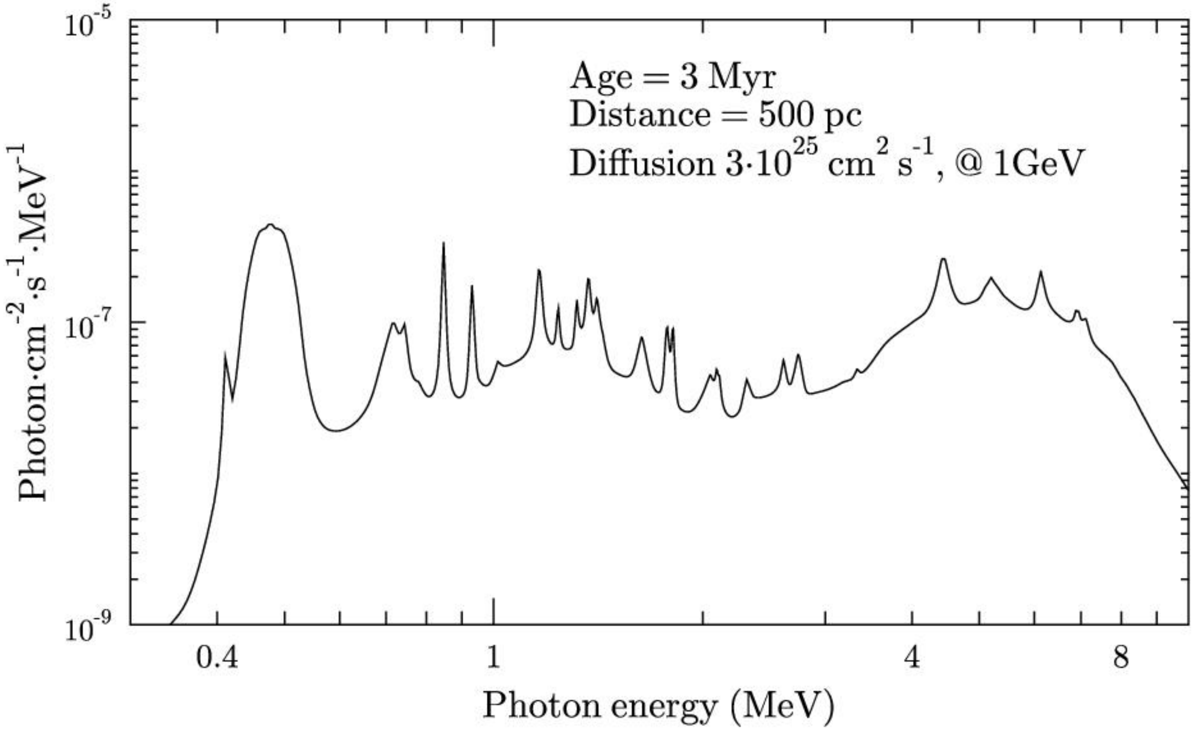

Sensitivity of ~ 10(-7) ph cm-2 s-1

Field of view ~ a few degrees

Pulsar Wind Nebulae

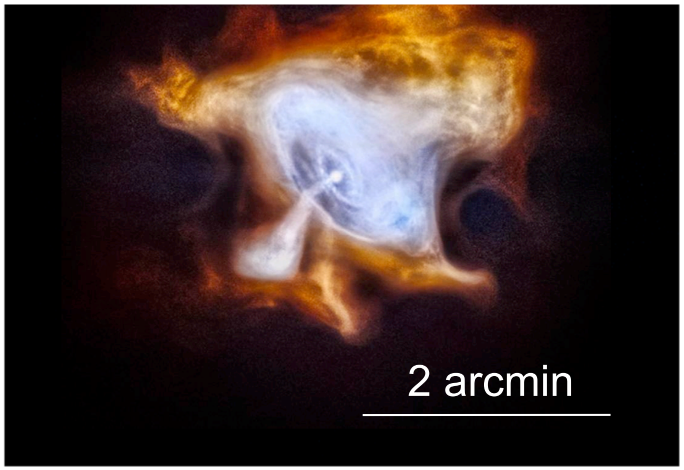
2 arcmin

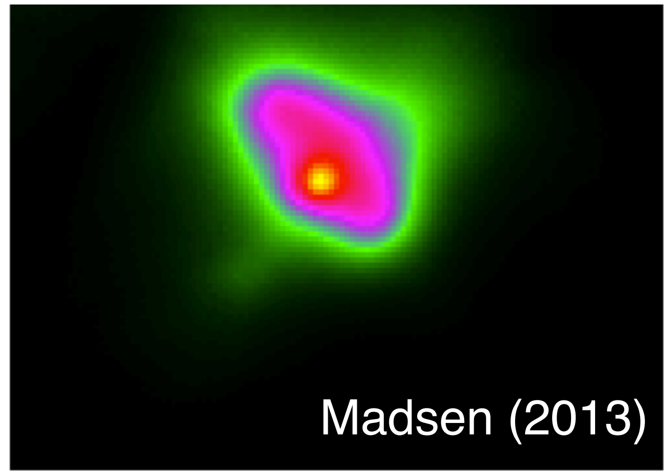
Madsen (2013)

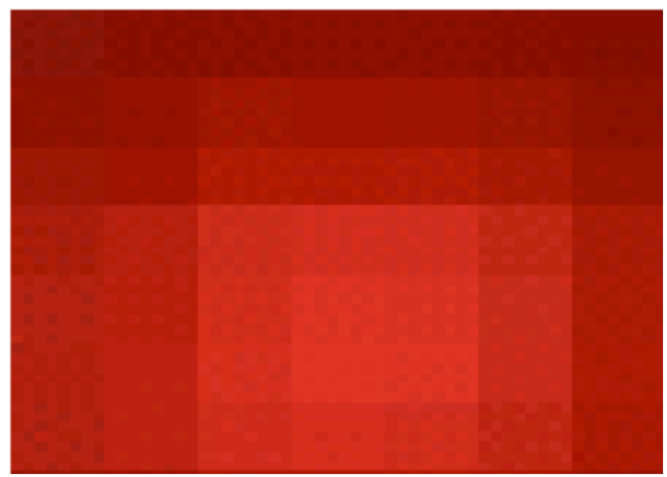

Crab Nebula

$$E_{syn} \sim 4(E_e/100\,\mathrm{TeV})^2(B/10^{-5}\,\mathrm{G})\ \mathrm{keV},$$

$$E_{ICS} \sim 1(E_e/20\,\mathrm{TeV})^2(\epsilon/6\times10^{-4}\,\mathrm{eV})\ \mathrm{TeV},$$

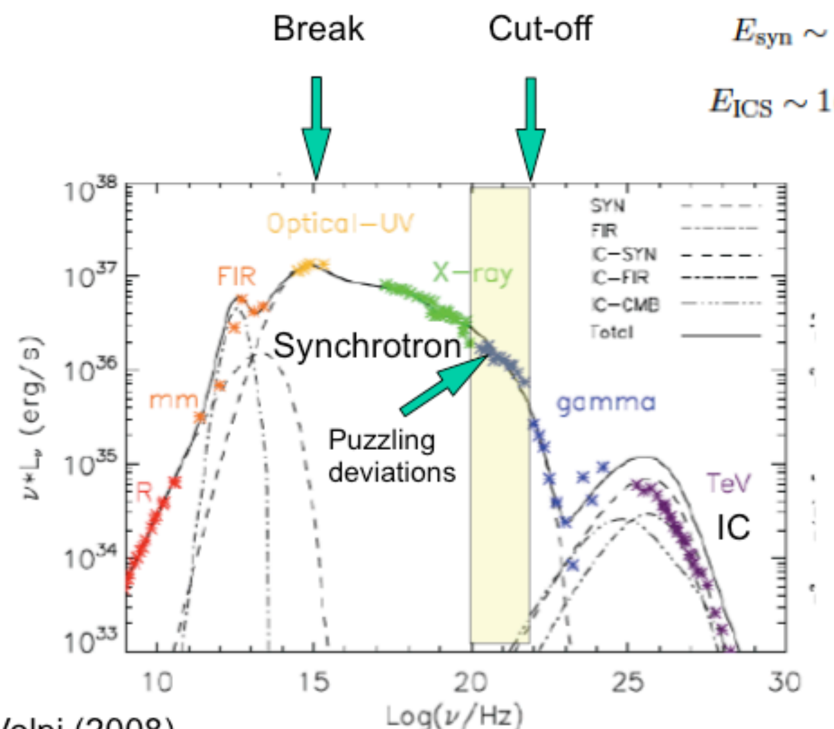

Volpi (2008)

References for the reported data are as follows: radio data are from Baars & Hartsuijker (1972); the mm data are from Mezger et al. (1986) and Bandiera et al. (2002); the infrared points are from IRAS in the far to mid-infrared (Strom & Greidanus 1992) and from ISO in the mid to near infrared range (Douvion et al. 2001); optical is from Véron-cetty & Woltjer (1993) and UV from Hennessy et al. (1992). Points in the range between soft X

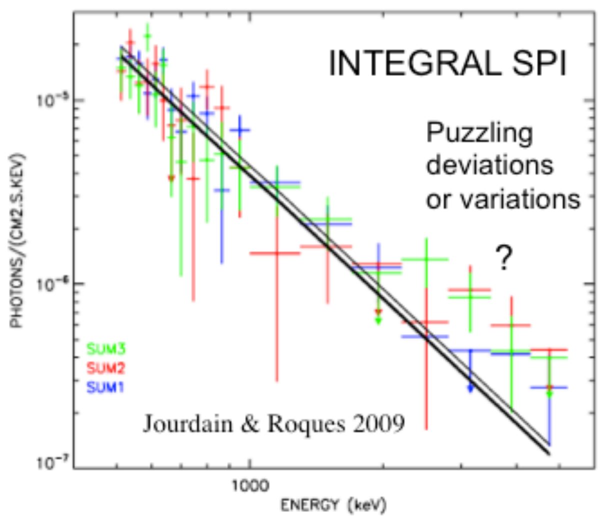

O.Kargaltsev

Vela X – PWN
two-components?

de Jager et al. 2008

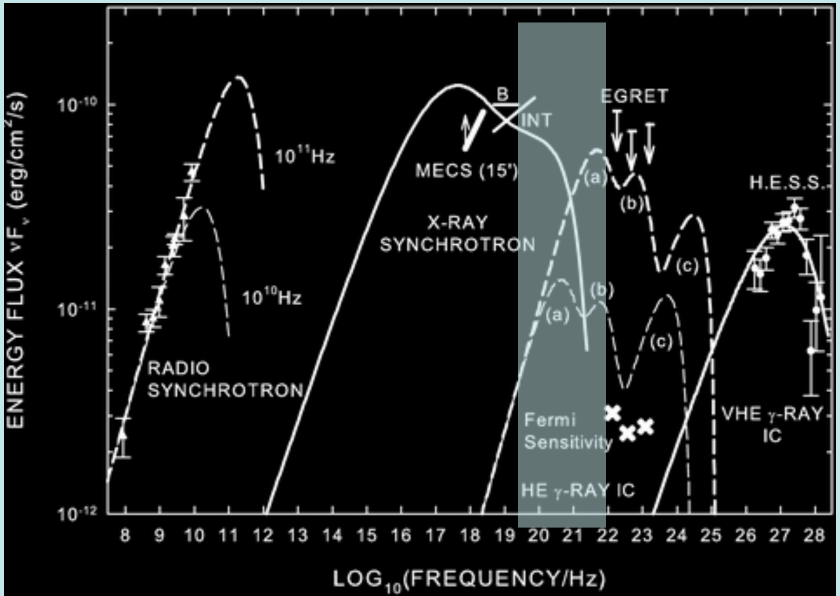

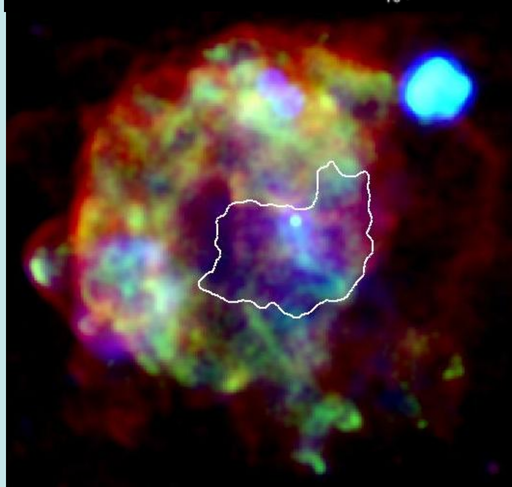

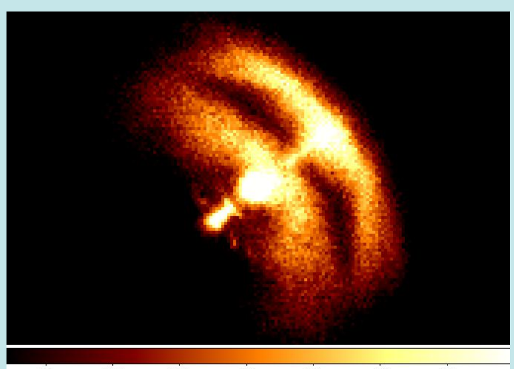

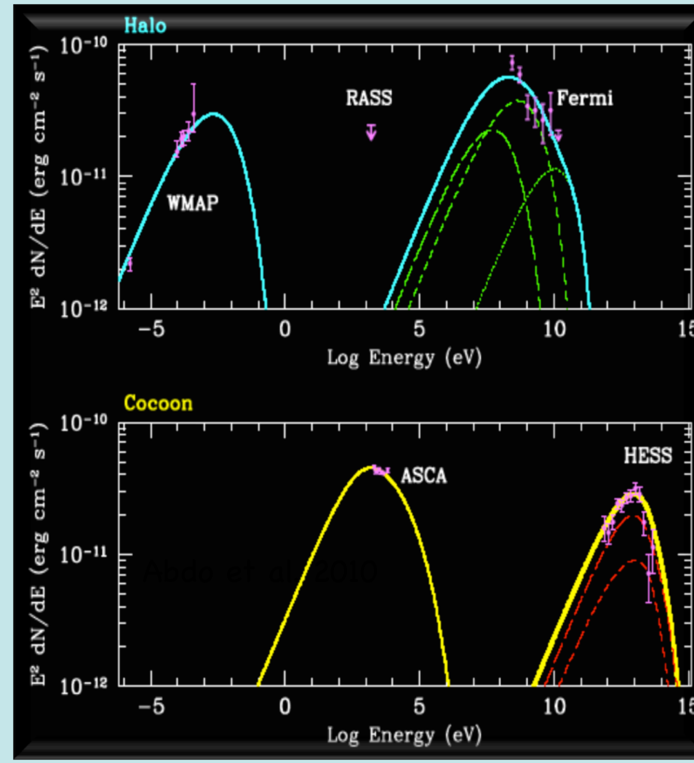

P.Slane

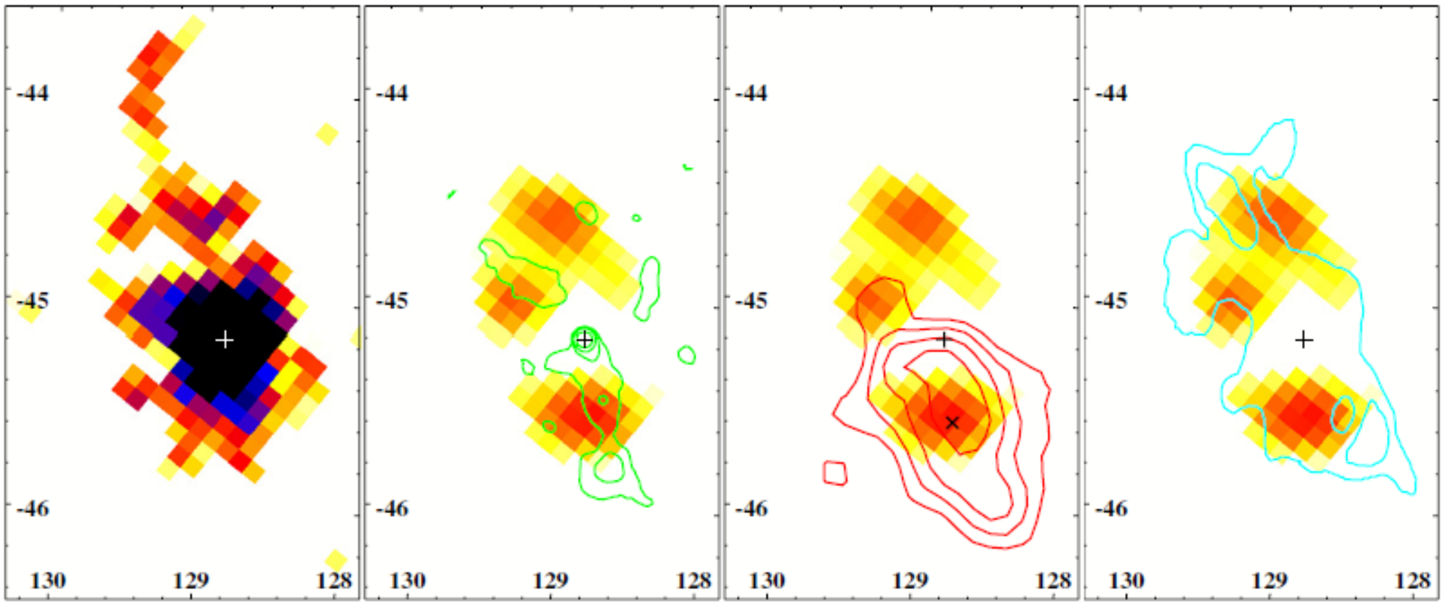

Figure 1. IBIS/ISGRI significance map in the 18–40 keV range (celestial coordinates, J2000; north is up, east is left). The color scale is chosen to highlight the faint emission. First panel: significance map; other panels: significance map after subtraction of the point-like source and smoothing with a 3 pixel ($\sigma \sim 7\farcm5$) Gaussian kernel. Contours: *ROSAT*, 0.5–2 keV (second panel, green); *H.E.S.S.*, VHE gamma-rays above 1 TeV (third panel, red; Aharonian et al. 2006); Spacelab 2, 2.5–12 keV (fourth panel, cyan; Willmore et al. 1992). The cross indicates the pulsar position. The X point in the third panel marks the best-fit center of gravity of the TeV emission.

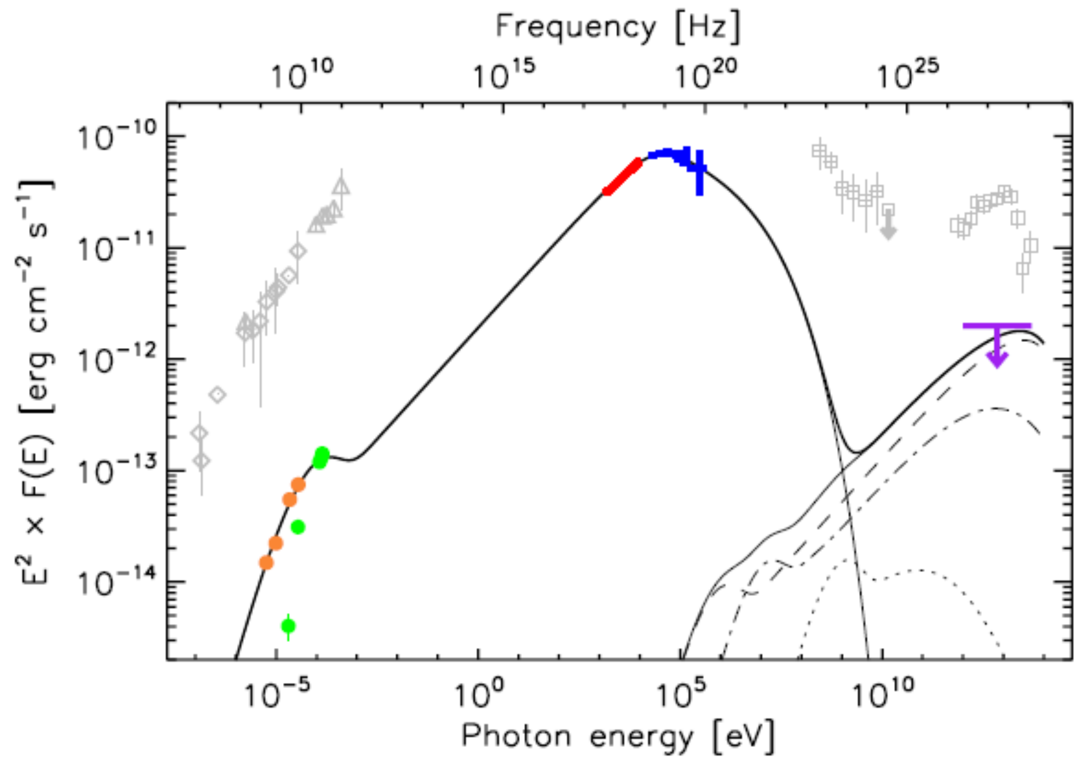

Figure 4. SED of the Vela PWN emission within 6′ from the pulsar, fitted with the model described in the text. The *Suzaku* XIS and *INTEGRAL* IBIS/ISGRI spectra are shown in red and blue, respectively. The radio fluxes of the inner Vela PWN are shown (Dodson et al. 2003; Hales et al. 2004, orange and green circles, respectively). The upper limit (99.9%) on the integral flux above 1 TeV within 6′ from the pulsar is also shown (purple arrow, assuming a photon index of 2; Aharonian et al. 2006). The measurements of the large-scale PWN are reported in gray for comparison: Vela X in radio (Alvarez et al. 2001; Abdo et al. 2010), at GeV energies (Abdo et al. 2010), and the TeV cocoon (Aharonian et al. 2006). The total (synchrotron and IC) model spectrum is indicated with a thick (thin) solid line. The IC emission is computed taking into account the CMB (dashed line), dust (dot-dashed line), and starlight (dotted line). The magnetic field is 10 μG.

VELA PWN RMHD Simulations

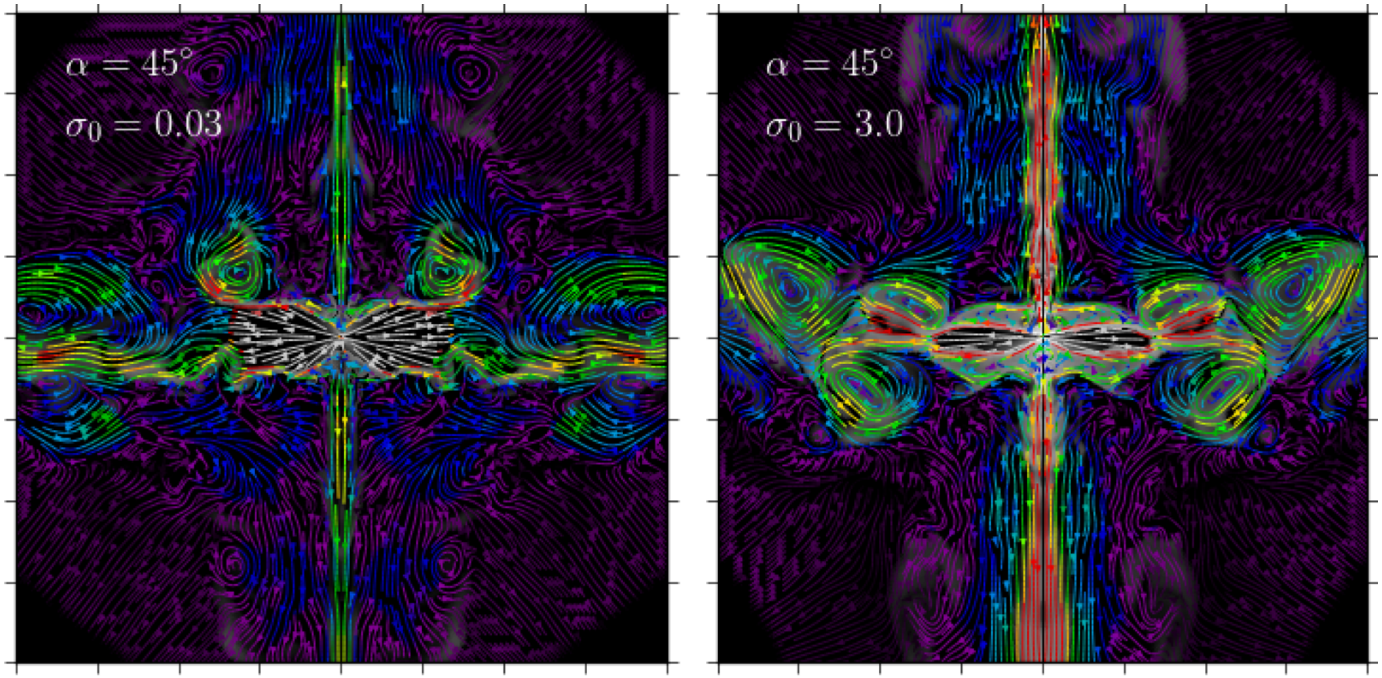

R.Buehler & M.Giomi 2016

A conservative scenario can be tested with eASTROGAM

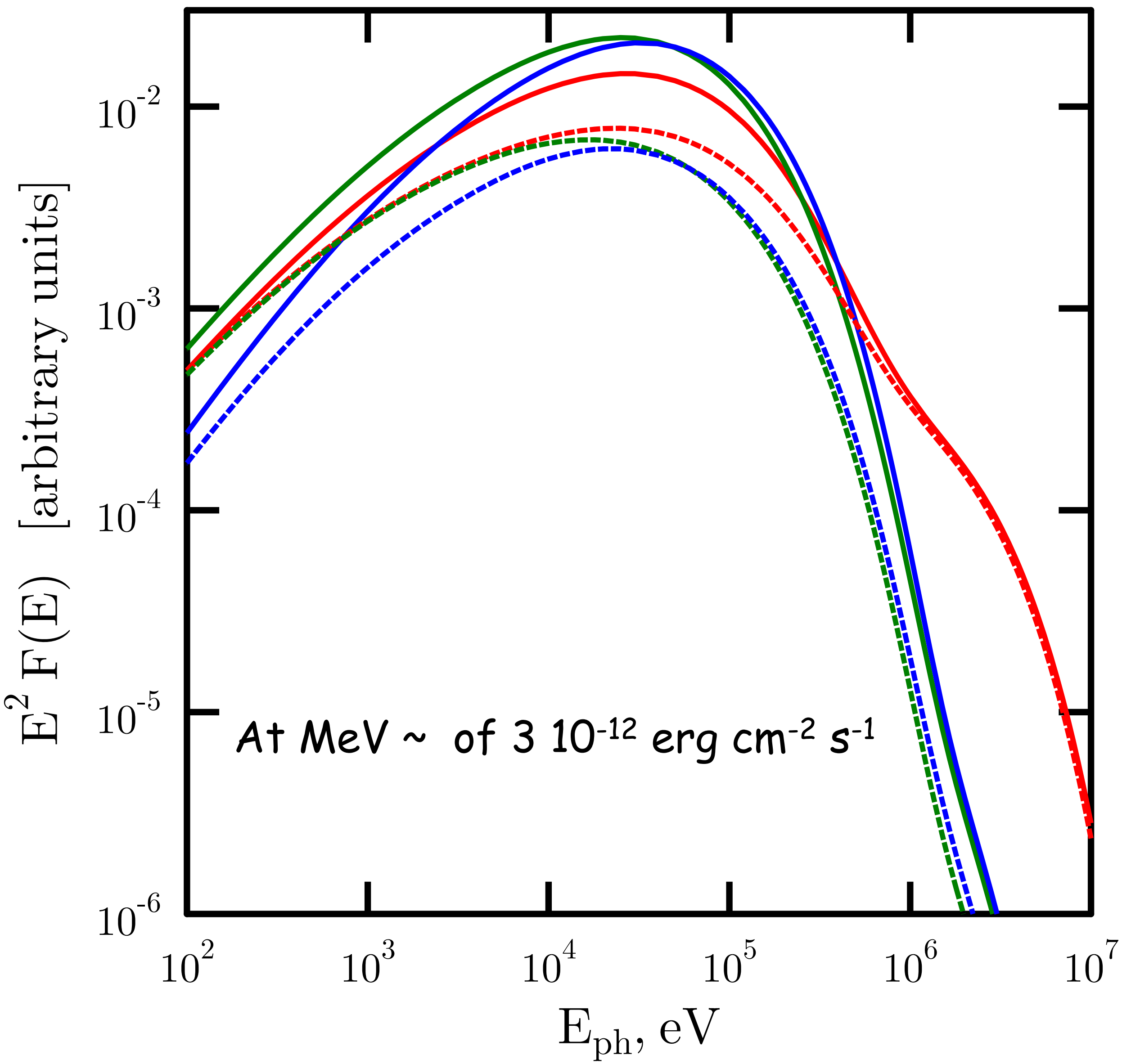

Thank You!